

# High Resolution Imaging with AEOS

*J. Patience, B.A. Macintosh, C.E. Max*

This article was submitted to  
The International Symposium on Optical Science and Technology,  
The International Society for Optical Engineering 47<sup>th</sup> Annual  
Meeting, San Diego, California, July 29 – August 3, 2001

**August 27, 2001**

**U.S. Department of Energy**

Lawrence  
Livermore  
National  
Laboratory

## DISCLAIMER

This document was prepared as an account of work sponsored by an agency of the United States Government. Neither the United States Government nor the University of California nor any of their employees, makes any warranty, express or implied, or assumes any legal liability or responsibility for the accuracy, completeness, or usefulness of any information, apparatus, product, or process disclosed, or represents that its use would not infringe privately owned rights. Reference herein to any specific commercial product, process, or service by trade name, trademark, manufacturer, or otherwise, does not necessarily constitute or imply its endorsement, recommendation, or favoring by the United States Government or the University of California. The views and opinions of authors expressed herein do not necessarily state or reflect those of the United States Government or the University of California, and shall not be used for advertising or product endorsement purposes.

This is a preprint of a paper intended for publication in a journal or proceedings. Since changes may be made before publication, this preprint is made available with the understanding that it will not be cited or reproduced without the permission of the author.

This report has been reproduced directly from the best available copy.

Available electronically at <http://www.doe.gov/bridge>

Available for a processing fee to U.S. Department of Energy  
and its contractors in paper from  
U.S. Department of Energy  
Office of Scientific and Technical Information  
P.O. Box 62  
Oak Ridge, TN 37831-0062  
Telephone: (865) 576-8401  
Facsimile: (865) 576-5728  
E-mail: [reports@adonis.osti.gov](mailto:reports@adonis.osti.gov)

Available for the sale to the public from  
U.S. Department of Commerce  
National Technical Information Service  
5285 Port Royal Road  
Springfield, VA 22161  
Telephone: (800) 553-6847  
Facsimile: (703) 605-6900  
E-mail: [orders@ntis.fedworld.gov](mailto:orders@ntis.fedworld.gov)  
Online ordering: <http://www.ntis.gov/ordering.htm>

OR

Lawrence Livermore National Laboratory  
Technical Information Department's Digital Library  
<http://www.llnl.gov/tid/Library.html>

# High Resolution Imaging with AEOS

Jennifer Patience<sup>1</sup>, Bruce A. Macintosh<sup>1</sup>, & Claire E. Max<sup>1</sup>

<sup>1</sup> Lawrence Livermore National Laboratory, 7000 East Ave. L-413, Livermore, CA 94550,  
patience@igpp.ucllnl.org, bmac@igpp.ucllnl.org, max@igpp.ucllnl.org

## ABSTRACT

The U. S. Air Force Advanced Electro-Optical System (AEOS) which includes a 941 actuator adaptive optics system on a 3.7m telescope has recently been made available for astronomical programs. Operating at a wavelength of 750 nm, the diffraction-limited angular resolution of the system is 0".04; currently, the magnitude limit is V~7 mag. At the distances of nearby open clusters, diffraction-limited images should resolve companions with separations as small as 4-6 AU – comparable to the Sun-Jupiter distance. The ability to study such close separations is critical, since most companions are expected to have separations in the few AU to tens of AU range. With the exceptional angular resolution of the current AEOS setup, but restricted target magnitude range, we are conducting a companion search of a large, well-defined sample of bright early-type stars in nearby open clusters and in the field. Our data set will both characterize this relatively new adaptive optics system and answer questions in binary star formation and stellar X-ray activity. We will discuss our experience using AEOS, the data analysis involved, and our initial results.

Keywords: adaptive optics, astronomy

## 1. INTRODUCTION

### 1.1 AEOS

The AEOS telescope is located on the Hawaiian volcano Haleakala, the highest point on the island of Maui. At an elevation of 10,000 ft., the site is above a convectively stable layer of air and compares favorably with many astronomical observatory sites in extinction, seeing, and fraction of clear nights (Kuhn et al. 1999). The telescope primary is a 3.67m diameter f/1.5 mirror with 132 actuators for active control of the mirror shape; details of the telescope and adaptive optics system reported in this section are taken from Berger et al. 1999. Two secondaries are available, providing a field-of-view of either 206" x 206" or 62" x 62" and requiring less than two hours to switch. Designed for satellite tracking, the telescope slew rate is exceptionally high, 17.6 deg/sec in azimuth and 4.75 deg/sec in elevation. Rather than employing a dome slit, the dome walls retract, increasing the range of observable targets and enhancing the temperature equilibration.

The aspect of the system most crucial to our program is the high order adaptive optics (AO) system designed to provide diffraction-limited resolution at optical wavelengths. The AO system optical path divides the light according to wavelength: the shortest wavelengths (<540 nm) are directed to the tip control subsystem consisting of a 5.3 cm Beryllium mirror and a 64 x 64 pixel CCD sensor; wavelengths from 540 – 700 nm pass through the wavefront sensor section. With a 32 x 32 lenslet array and 128 x 128 pixel CCD camera with frame rates of 500 – 5000 Hz, the wavefront sensor measures wavefront slopes and sends commands to correct the incident wavefront with a 28.8 cm diameter Xinetics 941 actuator deformable mirror. The deformable mirror thickness is 2 mm and the actuator stroke is  $\pm 2$   $\mu$ m. Because of the large number of actuators and rapid correction rate, AEOS is one of only a few systems that can operate at visible wavelengths. Although constructed for space surveillance programs, AEOS now serves the dual purposes of the military and the astronomical communities.

### 1.2 SCIENCE PROGRAM

Surveys of the both the nearest stars and star-forming regions have revealed a large fraction of binary stars -- ranging from ~60% to almost 100% -- and emphasize the importance of considering the binary environment in star and planet formation (Duquennoy & Mayor 1991, Ghez et al. 1993, Koehler & Leinert 1998, Simon et al. 1995). Despite the preponderance of multiple stars, the mechanism that produces multiple stars rather than single stars is still unknown. A variety of formation scenarios have been investigated, including fragmentation of the molecular cloud or circumstellar disk fragment to form a second star (*c.f.* Boss 1996), or binary formation from a capture process (*c.f.* McDonald & Clarke 1995). The mechanism by which a binary forms may critically affect the potential to form planetary systems and the properties of any resulting planets. In particular, formation by capture may strip stars of their circumstellar disks which provide a reservoir of material for planet formation. Observations of stars with a range of masses are important to test several models of binary star formation. A large set of solar-type stars have been observed in multiplicity surveys, however, substantially fewer early-type stars have been studied. The first goal of our project is

to obtain high resolution adaptive optics observations of a large sample of early-type stars in order to extend the mass range covered by binary star searches and to test binary formation theories.

In addition to providing insight into the star formation process, studies of companion stars may also explain the unexpected detection of X-ray emission from A stars. Stars along the entire Main Sequence, from massive O stars to M dwarfs, are detected as X-ray sources. Different mechanisms are believed to produce the X-ray emission of early-type (higher mass) and late-type (lower mass) stars – winds from massive stars and magnetic fields from the dynamo in less massive stars. Stars with spectral types of O and B have massive radiatively-driven winds which generate X-rays. The exact mechanism is uncertain, but proposed explanations include a thin high-temperature layer at the base of the corona (e. g. Cassinelli & Olson 1979) and shock-heated high density regions formed from instabilities in the wind (e.g. Lucy & White 1980). Beginning with spectral type F and continuing to M, stellar structure changes and a convective zone develops. Combined with stellar rotation, the convective motions maintain a dynamo which generates the surface magnetic fields and hence the loop structures that produce the X-rays of late-type dwarfs. This model for late-type stars is based on an analogy to the Sun (Cowling 1981). Since A stars lack both the strong winds of the earlier spectral types and the dynamos of the later spectral types, they are not expected to produce X-rays (Pallavicini 1989), however, some A stars are detected as X-ray sources. The second goal of our program is to investigate the possibility that companions may explain the unexpected X-ray emission from A stars.

Two models with different predictions for our observations have been suggested to account for the surprising X-ray detections of A stars. Binaries may be an important factor in the unexplained X-ray emission from these stars (e.g. Pallavicini 1989), since a later spectral type companion within the X-ray error box could produce the detected emission. Typical *ROSAT* (an X-ray satellite that mapped the entire sky) error boxes of  $\sim 10''$  are large enough to easily include a fainter companion. An alternate theory for the production of X-rays from A stars involves shearing motions in the coronae of these stars (Tout & Pringle 1994). The companion model suggests that X-ray A stars should exhibit a higher frequency of binaries, while the later model predicts that the binary fractions should be comparable. With the currently available cluster data (Patience et al. 2001), the fraction of binaries measured for X-ray detected A stars is higher than that of nondetected A stars, but the difference is only a two sigma result. The small sample of X-ray detected stars – 22 in total – limits the significance of the value; our observations will greatly increase the sample size and allow a more significant test of the theory.

## 2. SAMPLE

Young open clusters represent ideal laboratories for binary star studies, as they provide a set of stars with known ages and distances. One-half of the current sample for this research consists of the brightest members of two of the nearest open clusters – Coma Berenices and the Pleiades. To increase the total number of stars observed, we will also target X-ray detected A stars in the field. Of the 242 field X-ray A stars identified by Hunsch et al. (1998), 180 are observable with AEOS and we plan to obtain images of  $\sim 100$  stars.

The Pleiades cluster has been important for defining stellar age-activity relations (e.g. Stauffer & Soderblom 1991), conducting brown dwarf searches (Basri et al. 1996, Bouvier et al. 1998), and investigating binary star properties (Bouvier et al. 1997). Many recent studies of this cluster have concentrated on the solar-type and late-type stars, while this project involves a sample of early-type Pleiades members. The bright magnitudes of these stars make them ideal natural guide star AO targets.

Unlike the Pleiades, none of the Coma Berenices stars have been previously searched for companions with high-resolution techniques. Despite its nearby distance of only 81pc (Pinsonneault et al. 1998), making it the third-closest cluster, Coma Ber has been overlooked mainly because of its sparse population. Its members are unusual since they are almost exclusively early-type stars (Randich et al. 1996), a peculiarity that is beneficial to our program.

Both clusters also have a number of practical advantages for adaptive optics observing and for the AEOS system in particular. The declination of both clusters is  $\sim +25^\circ$ , placing them almost directly overhead in Hawaii. Although adaptive optics performance degrades at angles far from zenith, these clusters should not suffer from their location on the sky. Since Coma Ber and the Pleiades are among the nearest open clusters, a significant number of targets are brighter than the  $V \sim 8$  mag limit of the current AEOS system. The field stars provide another set of targets, often brighter than the cluster stars. Tables 1a-1c list the program stars that have been observed with AEOS. The object name, coordinates, V magnitude, (B-V) color, date of observation, and notes about X-ray detections are given.

## 3. OBSERVATIONS

AEOS observations were made during two observing runs on Nov 27-29, 2000 and April 25-27 2001 with the Visible Imager CCD camera (VISIM) on the AO bench. The camera operates over the 0.7 – 1.0  $\mu\text{m}$  wavelength range and has a 512 x 512 CCD array. Images were taken with a 700-800 nm or 700-1060 nm filter for the first run and with a Bessel I filter (similar to Johnson I) for the second run. Some of the brighter stars also required neutral density filters. Variable fields-of-view are possible with the VISIM camera:  $10''.5 \times 10''.5$ ,  $24''.7 \times 24''.7$ , and  $61''.8 \times 61''.8$ . For our program, the narrow and medium field were used to search the area around cluster and field A stars for stellar companions. The brightest star observed has a magnitude of

$V=2.9$  mag and the dimmest star observed has a magnitude of  $V=8.1$  mag, however, a more representative magnitude limit is  $V=7$  mag.

The observing strategy involved taking two types of images for each target. A set of 500 unsaturated narrow field exposures of 20-250 ms each were recorded to search for the closest companions. A large stack of images was taken in part to allow for the possibility of frame selection. Additionally, a smaller set of 10 -30 narrow or medium field saturated images were taken to search for wider, fainter companions. Since the cluster stars are of a similar magnitude and spread over a small region of the sky, stars detected as singles can be used as measures of the point spread function (PSF). The field X-ray A stars are located all over the sky and each requires a PSF calibration star; whenever possible, the PSF stars are chosen to have a similar magnitude and color as the target. During the first run, 18 Pleiades targets and 8 X-ray field stars and their PSFs were observed. Similarly, 17 Coma Ber members and 14 X-ray field stars and their associated PSF stars were observed during the second run. Since the observing periods are 6 hours rather than the full night, this efficiency is comparable to astronomical AO systems.

**Table 1a: Summary of Pleiades Observations**

Target	R.A (2000)	Dec (2000)	V	B-V	Date	Notes
Hz 447	3:44:48.1	24:17:26.9	5.5	0.0	27 Nov 2000	X-ray detection
Hz 717	3:45:37.7	24:20:12.9	7.2	0.2	28 Nov 2000	
Hz 801	3:45:48.9	23:08:54.2	6.9	0.0	28 Nov 2000	
Hz 817	3:45:54.4	24:33:20.9	5.8	0.0	27 Nov 2000	
Hz 859	3:46:02.9	24:31:44.4	6.4	0.0	27 Nov 2000	X-ray detection
Hz 980	3:46:19.5	23:56:53.1	4.2	-0.06	27 Nov 2000	
Hz 1234	3:46:59.2	24:31:16.9	6.8	0.0	28 Nov 2000	X-ray detection
Hz 1380	3:47:20.8	23:48:15.6	7.0	0.0	28 Nov 2000	X-ray detection
Hz 1375	3:47:21.0	24:07:02.6	6.3	0.0	28 Nov 2000	
Hz 1397	3:47:24.4	23:54:56.4	7.3	0.0	28 Nov 2000	
Hz 1431	3:47:29.4	24:17:22.1	6.8	0.1	28 Nov 2000	
Hz 1432	3:47:29.0	24:06:22.1	2.9	-0.1	27 Nov 2000	X-ray detection
Hz 1876	3:48:29.9	24:20:47.4	7.0	0.1	28 Nov 2000	
Hz 2168	3:49:09.7	24:03:17.0	3.6	-0.1	27 Nov 2000	
Hz 2181	3:49:11.0	24:08:16.9	5.1	-0.1	27 Nov 2000	
Hz 2263	3:49:21.6	24:22:55.3	6.6	0.0	28 Nov 2000	X-ray detection
Hz 2425	3:49:43.5	23:42:46.9	6.2	0.0	27 Nov 2000	
Hz 2507	3:49:58.0	23:50:59.0	6.7	0.1	28 Nov 2000	

**Table 1b: Summary of Coma Berenices Observations**

Target	R.A (2000)	Dec (2000)	V	B-V	Date	Notes
T10	12 10 46	27 16 55	6.04	0.11	26 April 2001	X-ray detection
T19	12 12 25	27 22 49	8.12	0.40	25 April 2001	
T60	12 19 02	26 00 29	6.48	0.18	25 April 2001	
T62	12 19 19	23 02 05	6.27	0.17	26 April 2001	X-ray detection
					25 April 2001	
					26 April 2001	
T82	12 21 27	24 59 49	7.42	0.28	26 April 2001	X-ray detection
T91	12 22 31	25 50 49	4.83	0.50	26 April 2001	
T104	12 24 03	25 51 03	6.73	0.24	25 April 2001	
T107	12 24 19	26 05 57	5.18	0.08	26 April 2001	X-ray detection
T109	12 24 27	25 34 57	6.39	0.27	25 April 2001	
T125	12 26 24	27 16 05	4.95	0.34	25 April 2001	
T130	12 26 59	26 49 35	5.00	0.08	27 April 2001	
					25 April 2001	
					27 April 2001	
T139	12 27 38	25 54 48	6.76	0.16	26 April 2001	
T144	12 28 39	26 13 37	6.54	0.18	25 April 2001	
T145	12 28 45	25 54 01	6.65	0.21	25 April 2001	
T146	12 28 55	25 54 49	5.29	-0.05	25 April 2001	
T160	12 31 01	24 34 03	5.46	0.05	25 April 2001	
T183	12 33 34	24 16 60	6.29	0.11	25 April 2001	

**Table 1c: Summary of Field X-ray A Star Observations**

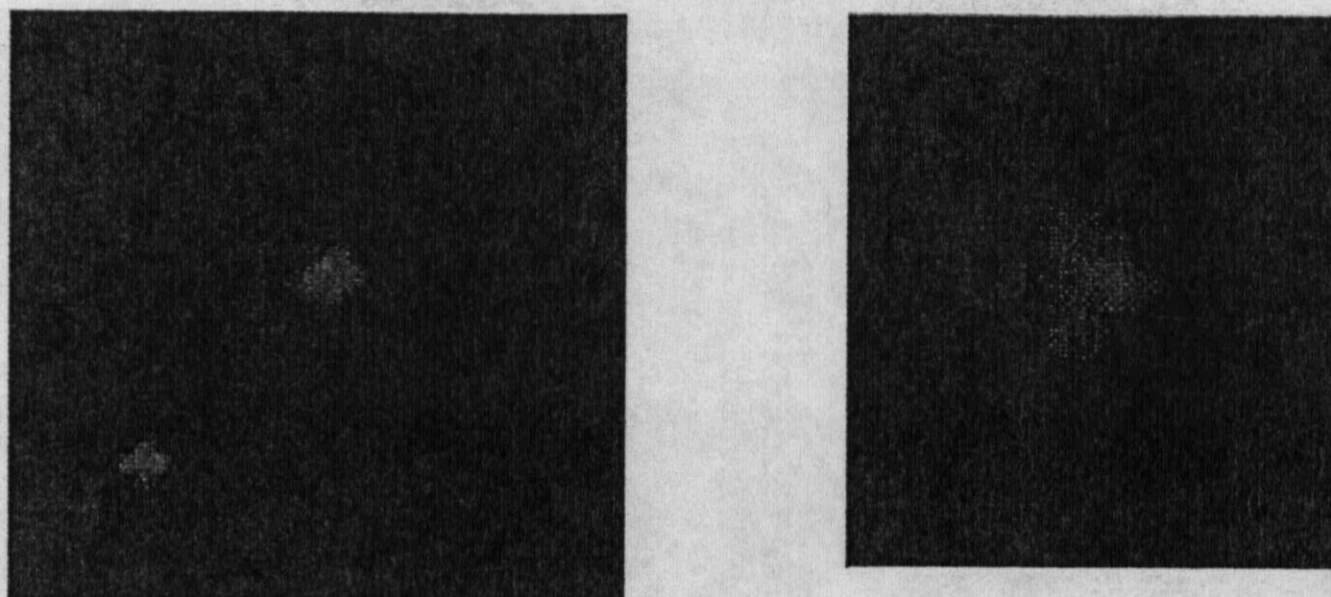
Target	R.A (2000)	Dec (2000)	V	B-V	Date	Notes
HR 328	01 07 57.2	20 44 20.8	5.55	0.13	29 Nov 2000	
HR 804	02 43 18.0	03 14 08.9	3.47	0.09	27 Nov 2000	
HR 943	03 07 50.8	-27 49 52.1	6.19	0.16	29 Nov 2000	
HR 971	03 15 20.4	30 33 24.1	5.52	0.01	29 Nov 2000	
HR 1697	05 12 48.1	-06 03 25.9	5.90	0.954	29 Nov 2000	PSF
HR 1839	05 30 47.1	05 56 53.3	4.20	-0.13	27 Nov 2000	PSF
HR 1940	05 39 31.2	-03 33 52.9	6.00	0.27	29 Nov 2000	
HR 2124	06 02 23.0	09 38 50.2	4.13	0.16	27 Nov 2000	
HR 2163	06 06 32.1	-23 06 39.0	5.46	0.07	29 Nov 2000	PSF
HR 2180	06 08 57.9	-22 25 38.7	5.50	-0.01	29 Nov 2000	
HR 2272	06 21 11.9	29 32 26.9	6.43	0.06	27 Nov 2000	
					29 Nov 2000	
HR 2298	06 23 46.1	04 35 34.3	4.41	0.18	27 Nov 2000	PSF
HR 2297	06 24 52.8	29 42 25.4	6.70	-0.06	29 Nov 2000	PSF
HR 2391	06 33 36.2	14 09 18.6	5.56	1.12	27 Nov 2000	PSF
HR 2383	06 33 42.7	33 01 26.5	6.53	0.05	27 Nov 2000	PSF
HR 3569	08 59 12.5	48 02 30.6	3.14	0.19	25 April 2001	
HR 3594	09 03 37.5	47 09 23.5	3.60	0.00	25 April 2001	PSF
HR 3690	09 18 50.6	36 48 09.3	3.82	0.06	25 April 2001	
HR 4096	10 27 28.0	41 36 03.7	6.02	0.17	26 April 2001	
HR 4113	10 30 06.4	38 55 30.5	5.79	0.08	26 April 2001	PSF
HR 4189	10 43 01.9	26 19 32.1	5.52	0.16	26 April 2001	PSF
HR 4203	10 45 51.9	30 40 56.3	5.24	-0.06	26 April 2001	
HR 4309	11 04 31.2	38 14 28.9	6.00	0.16	27 April 2001	PSF
HR 4380	11 19 07.9	38 11 08.0	4.78	0.10	25 April 2001	
					27 April 2001	
HR 4422	11 29 04.1	39 20 13.1	5.31	0.01	27 April 2001	
HR 4454	11 34 09.9	11 01 25.9	6.55	0.18	27 April 2001	
HR 4528	11 47 54.9	08 14 45.2	5.32	0.02	25 April 2001	
HR 4585	11 59 56.9	03 39 18.7	5.36	0.01	25 April 2001	PSF
HR 6332	17 01 36.4	33 34 05.8	5.25	0.02	27 April 2001	
HR 6436	17 17 40.3	37 17 29.4	4.65	0.05	27 April 2001	
HR 6554	17 32 10.6	55 11 03.3	4.88	0.26	27 April 2001	
HR 6555	17 32 16.0	55 10 22.7	4.87	0.28	27 April 2001	
HR 7051	18 44 20.4	39 40 12.2	5.06	0.16	27 April 2001	

#### 4. PRELIMINARY RESULTS

##### 4.1 RESOLUTION AND SENSITIVITY

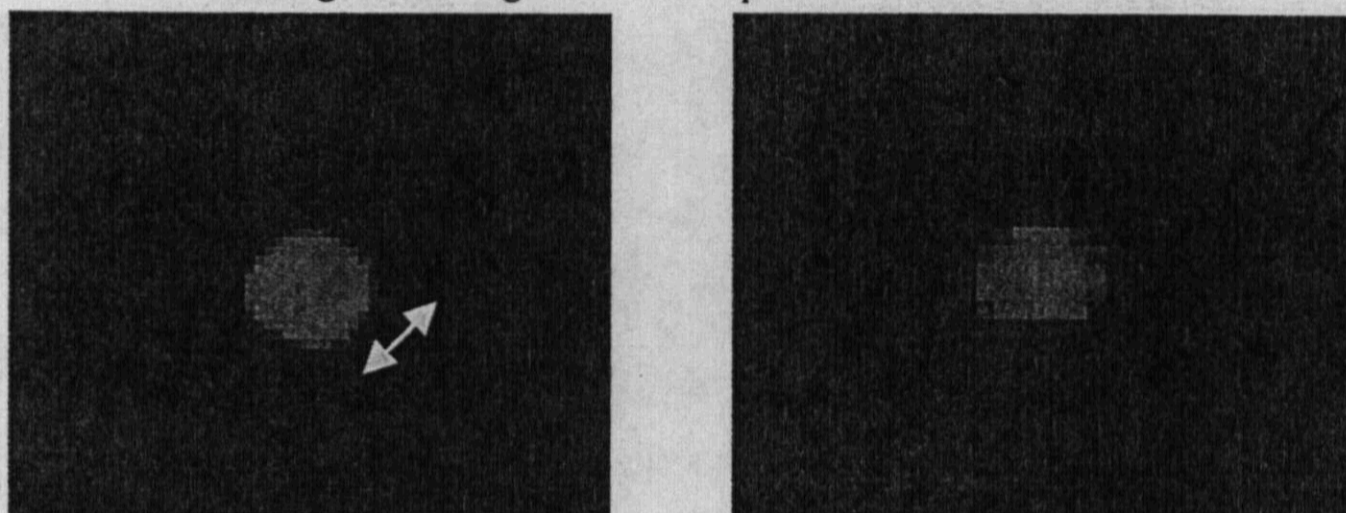
The image quality varied considerably with different conditions. During the first run, marked by higher winds and unstable performance of the AO system, the typical point spread function showed multiple lobes and varied appreciably. Wider systems are easily detectable as seen in Figure 1a, but the shape of the point spread function, shown in Figure 1b, severely limits the ability to detect subarcsecond binaries, a requirement for our program. During the second run, the winds were lower and the dome sides remained raised to further reduce windshake. Operating the telescope with only the roof retracted limits the elevation range to within 30 degrees of zenith, but that did not impact the majority of the observations. An example 0".2 binary is shown in Figure 2a and a typical point spread function in Figure 2b; the images are sharper and more symmetric than those from the first run. Typical image artifacts, common to both runs, are shown in Figure 3.

Figure 1: Images from the Nov. 2000 AEOS Run



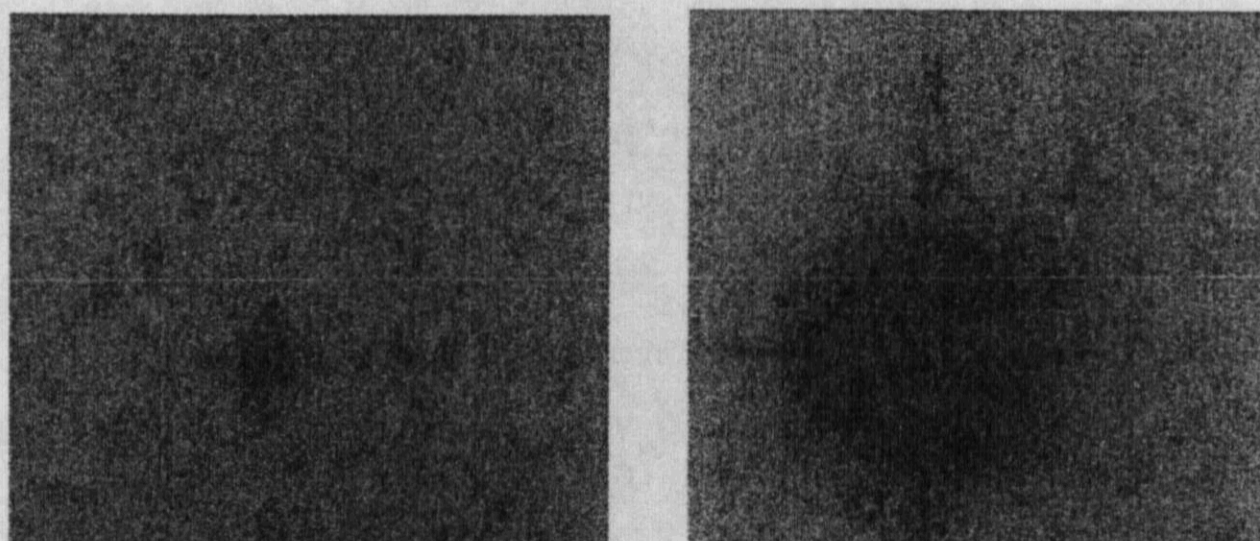
The image on the left (1a) is an example of the wide binaries detectable with this dataset. As seen in the image on the right (1b), the shape of the point spread function prevents the detection of very close companions.

Figure 2: Images from the April 2001 AEOS Run



These images show the improved data quality of the second dataset. The image on the left (2a) reveals a  $0''.2$  companion which would have been difficult to distinguish in the data from the November run. On the right (2a), is a typical point spread function.

Figure 3: Common VISIM Image Artifacts

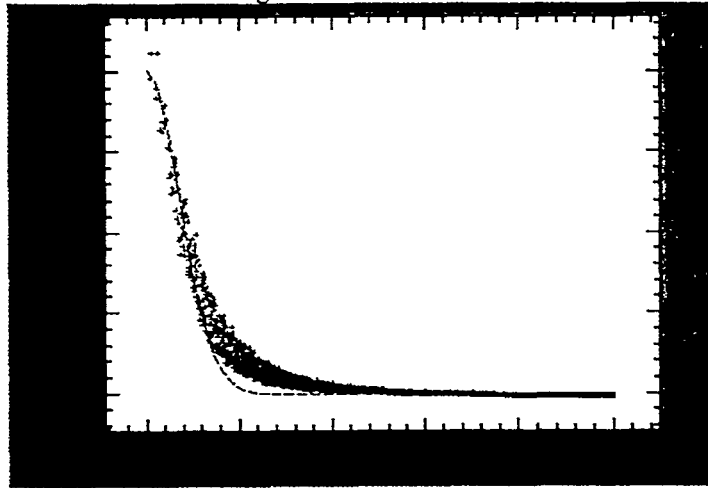


These color inverted images show artifacts common to the short and long exposure images. On the left, a short exposure image (3a) shows the four bright points caused by waffle mode on the deformable mirror. The deep exposure on the right (3b) appears to have a companion at 315 degrees East of North (North is up and East is to the left), but this is a ghost reflection.

A radial profile of the combination of many 200 ms unsaturated images from the second run is given in Figure 4. The FWHM is 6.5 pixels or  $0''.13$ , slightly less than 3 times the diffraction limit of  $0''.048$  at the central wavelength of the filter  $\sim 0.85 \mu\text{m}$ . Although not diffraction-limited, the shorter unsaturated exposures allow detection of subarcsecond companions. The detection limit of the short and long exposure images are determined by calculating the flux ratio corresponding to an object 5 sigma above the noise level and the target star. The current radial profile

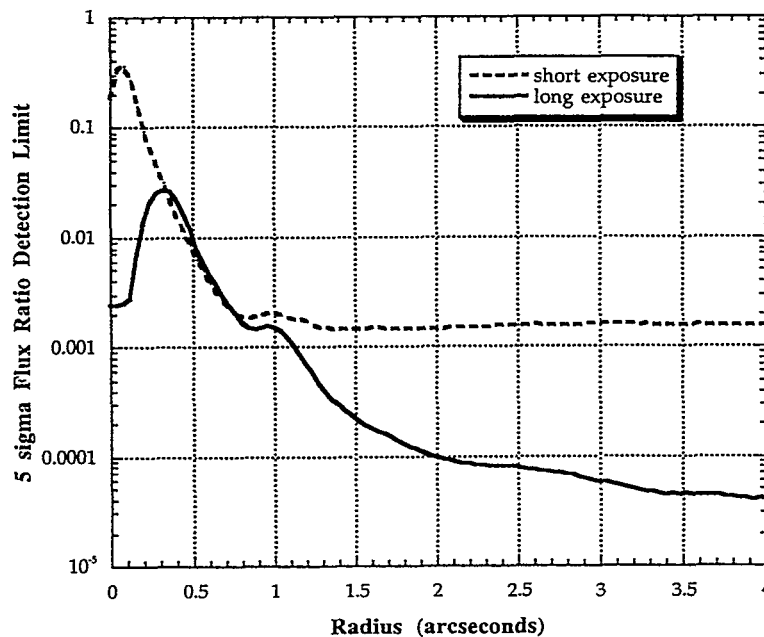
and sensitivity limits do not involve images that have been selected based on higher Strehl ratios; given the seeing fluctuations and variable AO performance, frame selection may significantly sharpen the final images and improve the limits. Figure 5 shows the companion detection limits as a function of angular separation from the target star; the short exposure images have the better limits for subarcsecond companions, while the longer exposure times make the deeper images more sensitive to wide companions. The observable contrast ratios improve significantly with radius: 10 times fainter at  $0''.2$ , 150 times fainter at  $0''.5$ , 1,000 times fainter at  $1''.0$ , and 10,000 times fainter at  $2''.0$ . For an A5 target star, G star companions are detectable beginning at a separation of  $0''.2$  and M star companions at separations of  $0''.5$  or larger. All possible stellar companions could be imaged for  $2''$  or wider systems.

Figure 4: Radial Profile



This figure shows the radial profile of the combination of a stack of 500 images, each with an exposure time of 200ms. The FWHM of the image is 6.5 pixels which corresponds to  $0''.13$ , 2.7 times the diffraction limit in the I-band. The target is the Coma Berenices member T139.

Figure 5: Detection Limits for Unseen Companions



The 5 sigma detection limits for companion stars are plotted as a function of angular separation from the target star.

## 4.2 A STAR BINARY FRACTION

Companion stars to many of the A stars are resolved by the AEOS images. Currently, only data from the second run have been analyzed systematically for companions. Examples of the resolved systems are shown in Figure 7. All of the primaries included in Figure 7 are X-ray detected stars and the companions are all within the ROSAT error box and could account for the X-ray detection. Follow-up infrared observations are planned to measure the (I-K) color of the companions to determine if the stars are physically associated and to estimate the spectral type of the second star in the field. Among the stars analyzed thus far, there is a high fraction of binaries in the X-ray detected stars. Although the sample is very small, 8 of 11 X-ray detected field or cluster stars are binary, while none of the 6 cluster stars without an X-ray identification has a companion.

Figure 7: Binary X-ray A Stars



Three examples of the binaries resolved with AEOS are given in this figure. On the left is the Coma Berenices X-ray A star T 107. The middle image shows the field X-ray A star HR 6332 and the right images displays the field X-ray A star HR 7051. None of these targets are listed as known binaries in the Coma Ber X-ray survey or the ROSAT cross-correlation with the Bright Star Catalogue. None of the stars without X-ray emission are resolved as binary stars.

## 5. SUMMARY & FUTURE WORK

In summary, we have obtained AO images of 36 cluster and 22 field stars during two observing runs with the 3.67m AEOS telescope which was recently made available for astronomical projects. A basic image reduction of the majority of the second run data is complete. Based on these preliminary results, the FWHM of the images is 6.5 pixels or  $0''.13$ . For comparison, the diffraction limit of a 3.67m telescope operating at a wavelength of  $0.85 \mu\text{m}$  (center of I-band filter) is  $0''.048$ . The 5 sigma detection limits as a function of separation are calculated. At close separations of  $0''.2$  companions  $\sim 10$  times fainter or spectral type early G are detectable and by  $0''.5$  companions  $\sim 150$  times fainter or spectral types of early M can be distinguished; finally, all possible stellar companions are detectable outside  $2''.0$ . Although based on a very small number of targets at this point, the proportion of binaries with X-ray detections is high – 8/11 – compared to 0/6 for stars without X-ray emission. Several steps remain incomplete: the separations and magnitude differences of all the binaries have to be carefully measured. For more significant statistics, a larger sample size is needed. There are 180 field X-ray A stars with declinations within the range of the AEOS telescope and we have proposed to observe 100 of them.

## ACKNOWLEDGEMENTS

We thank Lewis Roberts, Chris Neyman, Paul Kervin, and the AEOS observatory staff for their support of our observations. We also gratefully acknowledge funding from the Air Force Office of Scientific Research. This work was performed under the auspices of the US Department of Energy by the University of California Lawrence Livermore National Laboratory under contract W-7405-ENG-48.

## REFERENCES

- Basri, G., Marcy, G. W., & Graham, J. R. 1996, *ApJLett*, 469, 53.
- Berger, P. J. et al. 1999, The 1999 AMOS Technical Conference, Kihei, HI, 30 Aug – 3 Sep 1999.
- Bouvier, J., Stauffer, J. R., Martin, E. L., Barrado y Navascues, D., Wallace, B., & Bejar, V. J. S. 1998, *A&A*, 336, 490.
- Bouvier, J., Rigaut, F., & Nadeau, D. 1997, *A&A*, 323, 139.
- Boss, A. P. 1996, *ApJ*, 468, 231.
- Cassinelli, J. P. & Olson, G. L. 1979, *ApJ*, 229, 304.
- Cowling, T. G. 1981, *ARAA*, 19, 115.

- Duquennoy, A. & Mayor, M. 1991, A&A, 248, 485.
- Ghez, A. M., Neugebauer, G., & Matthews, K. 1993, AJ, 106, 2005.
- Hunsch, M., Schmitt, J. H. M. M., & Voges, W. 1998, A&ASS, 132, 155.
- Koehler, R. & Leinert, Ch. 1998, A&A, 331, 977.
- Kuhn, J. R., Waterson, M., Northcott, M., Maberry, A., Tokunaga, A. 1999, The 1999 AMOS Technical Conference, Kihei, HI, 30 Aug – 3 Sep 1999.
- Lucy, L. B. & White, R. L. 1980, ApJ, 241, 300.
- McDonald, J. M. & Clarke, C. J. 1995, MNRAS, 275, 671.
- Pallavicini, R. 1989, A&A Rev., 1, 177.
- Patience, J., Ghez, A. M., & Reid, I. N. 2001, AJ, submitted.
- Pinsonneault, M. H., Stauffer, J., Soderblom, D. R., King, J. R., & Hanson, R. B. 1998, ApJ, 504, 170.
- Randich, S., Schmitt, J. H. M. M., Prosser, C. 1996, A&A, 313, 815.
- Simon, M., Ghez, A. M., Leinert, Ch., Cassar, L., Chen, W. P., Howell, R. R., Jameson, R. F., Matthews, K., Neugebauer, G., & Richichi, A. 1995, ApJ, 443, 625.
- Stauffer, J. R. & Soderblom, D. R. 1991, in *The Sun in Time*, eds. Sonett, C. P., Giampapa, M. S. & Matthews, M. S.
- Tout, C. A. & Pringle, J. E. 1994, MNRAS, 272, 528.